# MÖBIUS MAPS AND CONTINUED FRACTIONS

**Carminda M. Mennen**
*School of Mathematics, University of the Witwatersrand, Johannesburg, South Africa*
carminda.mennen@wits.ac.za

*Received: 6/9/23, Accepted: 5/15/24, Published: 5/20/24*

**Abstract**

The connection between the partial quotients of the regular continued fraction and the number of left and right cuts of the cutting sequence of a geodesic across the triangles of the Farey tessellation has been established by Series. To find a similar connection for the nearest integer continued fraction, we require a completely new approach that combines aspects of well-known work on continued fractions. Firstly, we discuss the impact of actually truncating the continued fraction and explore alternate methods that use Möbius maps. We then animate the roles of various vertices, geodesics, and Farey triangles, in the geometrical figures that are commonly used, by developing a geometrical animation of the process that underlies the continued fraction of an irrational real number $\xi$. Finally, we reveal the interplay between the orbits of three vertices, namely zero, one, and infinity, as they move toward $\xi$, through rational values, under the action of successive partial products of Möbius maps derived from the nearest integer continued fraction.

## 1. Introduction

Any irrational number $\xi$ has an infinite continued fraction representation,

$$\xi = b_0 + \cfrac{1}{b_1 + \cfrac{1}{b_2 + \ddots}} = [b_0, b_1, b_2, \cdots], \tag{1}$$

where the partial quotients $b_k$ satisfy $b_0 \in \mathbb{Z}, b_k \in \mathbb{N}$ for $k \in \mathbb{N} = \{1, 2, 3 \cdots\}$, if it is derived from the Euclidean algorithm [8], but $b_k \in \mathbb{Z}$ if the nearest integer algorithm is used. The continued fraction of Equation (1) is call a *regular continued fraction* $(RCF)$ in the former case and a *nearest integer continued fraction* $(NICF)$ in the latter. Traditionally, one finds rational approximants of $\xi$ by truncating the

DOI: 10.5281/zenodo.11221703

continued fraction at the nth partial quotient $b_n$ to get convergents $C_n = \frac{p_n}{q_n} = [b_0, b_1, \cdots, b_n]$, determined as a rational in reduced form. We sacrifice accuracy for speed [7] when generating approximants by truncating the $NICF$ instead of the $RCF$. We use Beardon's suggestion [3, 4, 6] to analyze the behavior of continued fractions in hyperbolic space where Möbius maps act as isometries.

In this paper, we compare the process for the $RCF$ and the $NICF$. We give notation and basic definitions in Section 2. In Section 3, we use a new dynamic approach to show how parabolic Möbius maps derived from a continued fraction link the partial quotients of the continued fraction and the triangles of the Farey tessellation when $\xi \in \mathbb{R}$ has $NICF = RCF$. In Section 4, we consider $\xi$ with $NICF \neq RCF$. The roles of geometric elements evolve and the dynamic is adapted accordingly. We link the number of triangles of the Farey tessellation directly to the coefficients of the Möbius maps derived from the $NICF$ in Section 5. Continued fractions of quadratic surds always have periodic partial quotients, a result discussed in the work of Beardon in [6]. This periodicity will not affect the generality of the discussion in this paper. We state our main theorem in Section 6, describing the link between the partial quotients of the $NICF$ and the triangles of the Farey tessellation of hyperbolic space. In Section 7, we briefly discuss further areas of research.

## 2. Basic Notation and Definitions

We introduce the geometry underpinning the $NICF$ in terms of Möbius maps acting on hyperbolic space.

### 2.1. The Farey Tesselation of Hyperbolic Space

The Farey tessellation $\mathcal{F}$, used by Series [13] in 1985, is a tiling of the upper half plane model of hyperbolic space $\mathbb{H}$ into hyperbolic triangles, where $\mathbb{H} = \{z \in \mathbb{C} : Im(z) > 0\}$ is endowed with the Poincare metric $ds^2 = \frac{dx^2+dy^2}{y^2}$. The closure of $\mathbb{H}$ includes the extended real line $\mathbb{R}_\infty = \mathbb{R} \cup \{\infty\}$ (the circle at infinity) as the boundary $\partial\mathbb{H}$. The following properties [8] hold in the Farey tessellation $\mathcal{F}$ of $\mathbb{H}$.

- Each endpoint of a Farey geodesic represents a reduced rational with denominator in $\mathbb{N}_0 = \mathbb{N} \cup \{0\}$.
- All geodesics are Farey geodesics $\lambda_{\left(\frac{a}{b}, \frac{c}{d}\right)}$ joining reduced rational endpoints $\frac{a}{b}$ and $\frac{c}{d}$ (with $a, b, c, d \in \mathbb{Z}$ and $b, d > 0$). The endpoints are Farey neighbors, denoted $\frac{a}{b} \sim \frac{c}{d}$, as the Farey neighbor condition $|ad - bc| = 1$ is satisfied.

- The three vertices of a triangle $\left(\frac{a}{b}, \frac{e}{f}, \frac{c}{d}\right)$ in $\mathcal{F}$, with $\frac{a}{b} < \frac{e}{f} < \frac{c}{d}$, satisfy the Farey sum condition $\frac{e}{f} = \frac{a}{b} \oplus \frac{c}{d} = \frac{a+c}{b+d}$. Since $\frac{a}{b} \sim \frac{c}{d}$, $\frac{a}{b} \sim \frac{e}{f}$, and $\frac{e}{f} \sim \frac{c}{d}$, all triangles in $\mathcal{F}$ are Farey triangles bounded by three Farey geodesics.

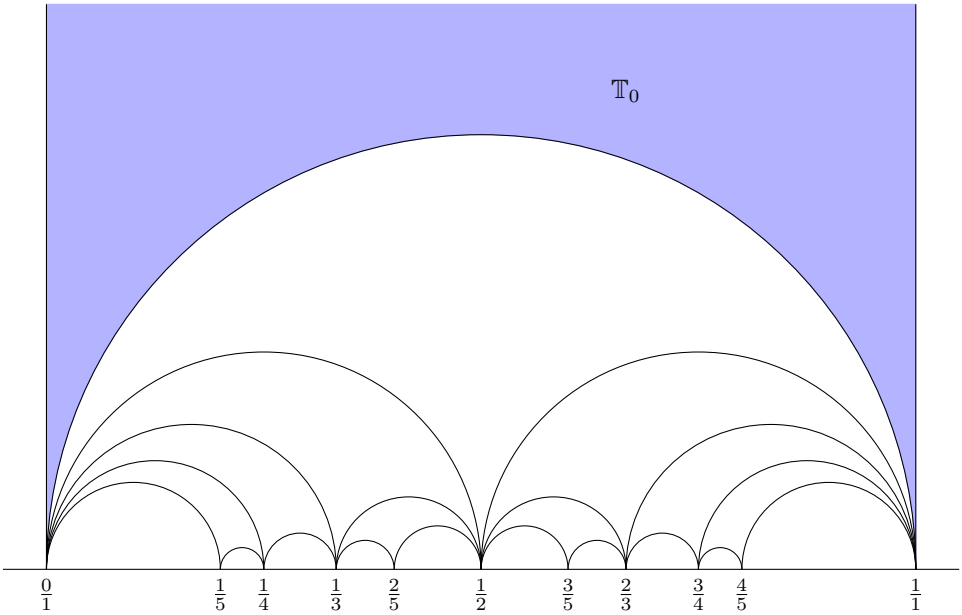


Figure 1: The Farey tessellation of $\mathbb{H}$ and the fundamental triangle $\mathbb{T}_0$.

In the diagram of Figure 1, we introduce the fundamental triangle $\mathbb{T}_0$ which is the shaded hyperbolic triangle with vertices 0, 1, and $\infty$ that are joined pairwise by Farey geodesics. The vertical lines $z = 0$ and $z = 1$ are Farey geodesics joining the vertex at $\infty$ to the vertices at 0 and 1, respectively. The part of $\mathcal{F}$ shown in the diagram of Figure 1 consists of all ideal geodesics joining Farey neighbors $\frac{a}{b}$ and $\frac{c}{d}$, with $0 \leq \frac{a}{b}, \frac{c}{d} \leq 1$ and $0 \leq b, d \leq 5$.

### 2.2. The Action of Möbius Maps in Hyperbolic Space

We define Möbius maps as follows, and discuss how they are central to our analysis.

**Definition 1.** *Möbius maps* are functions of the form $g(z) = \dfrac{az+b}{cz+d}$, $a, b, c, d \in \mathbb{C}$ with $ad - bc \neq 0$, which map the extended complex plane $\mathbb{C}_\infty = \mathbb{C} \cup \{\infty\}$ onto itself with $g(\infty) = \dfrac{a}{c}$ and $g\left(\dfrac{-d}{c}\right) = \infty$.

In the work of Beardon [6], the Möbius map $g(z) = \dfrac{(b_0b_1+1)\,z + b_0}{b_1 z + 1}$ expresses the continued fraction

$$f(z) = b_0 + \cfrac{1}{b_1 + \cfrac{1}{z}}.$$

We convert the continued fraction $[b_0, b_1, \cdots]$ into the product of maps $T = \tau_{b_0}\phi\tau_{b_1}\phi\tau_{b_2}\cdots$, where $\tau_{b_k}(z) = b_k + z$ (with $k \in \mathbb{N}_0 = \mathbb{N} \cup \{0\}$) and $\phi(z) = \dfrac{1}{z}$. These are both Möbius maps, where $\tau_{b_k}$, with $ad-bc = 1$, leaves the hyperbolic plane $\mathbb{H} = \{z \in \mathbb{C} : Im(z) > 0\}$ invariant, but $\phi$, with $ad - bc = -1$, interchanges the upper half-plane $\{z \in \mathbb{C} : Im(z) > 0\}$ with the lower half-plane $\{z \in \mathbb{C} : Im(z) < 0\}$, while leaving $\mathbb{R}_\infty$ invariant [9].

The modular group $\Gamma = \left\{z \mapsto \frac{az+b}{cz+d} : ad - bc = 1,\ a, b, c, d \in \mathbb{Z}\right\}$ contains the isometries of the hyperbolic plane [6, 8], so we wish to use only elements of $\Gamma$. In order to achieve this, we parse the maps of $T$ into the alternate factors $\tau_{b_k}$ and $\phi\tau_{b_k}\phi$, where $\phi\tau_{b_k}\phi(z) = \dfrac{z}{b_k z + 1}$, so $\phi\tau_{b_k}\phi \in \Gamma$.

The classification of Möbius maps requires that every $g(z) = \frac{az+b}{cz+d} \in \Gamma$ be represented by a normalized matrix. We represent $g$ by $A = \left(\begin{smallmatrix} a & b \\ c & d \end{smallmatrix}\right)$ since $ad - bc = 1$ for $g \in \Gamma$. Using the work of Beardon [2] and Anderson [1], we classify Möbius maps as follows.

**Definition 2.** Let $g$ be a Möbius transformation in $\Gamma$ with associated normalized matrix $A = \left(\begin{smallmatrix} a & b \\ c & d \end{smallmatrix}\right)$. Then:

i) $g$ is *parabolic* if and only if $tr^2(A) = 4$ if and only if $g$ has a unique fixed point in $\partial\mathbb{H}$;

ii) $g$ is *elliptic* if and only if $0 \le tr^2(A) < 4$ if and only if $g$ has a unique fixed point in $\mathbb{H}$;

iii) $g$ is *loxodromic (hyperbolic)* if and only if $tr^2(A) > 4$ if and only if $g$ has two fixed points in $\partial\mathbb{H}$.

Since all possible values for $tr^2(A)$ are exhausted in Definition 2, these three types of Möbius maps are the only possible types of Möbius maps found in $\Gamma$.

In the following definition, we rewrite $T$ as a product of parabolic Möbius maps whose factors alternate between the maps $\tau_{b_n}$ and $\phi\tau_{b_n}\phi$, that fix $\infty$ and 0, respectively. We also define $T_n$, the partial product of parabolic Möbius maps, as follows.

**Definition 3.** Let $[b_0, b_1, b_2, \cdots]$ be the *RCF* (or *NICF*) for some irrational number $\xi$. We let $T = t_0t_1t_2\cdots$ be the *product of parabolic Möbius maps associated with the RCF (or NICF) of* $\xi$, with $t_k = \tau_{b_k}$ for $k$ even and $t_k = \phi\tau_{b_k}\phi$ for $k$ odd,

where $b_k \in \mathbb{N}$ (or $b_k \in \mathbb{Z}$) for each $k \in \mathbb{N}_0$. We call $T_n = t_0 t_1 \cdots t_n$ the *partial product of parabolic Möbius maps of the RCF (or NICF) of* $\xi$ and it has $n+1$ factors.

Since $\frac{m}{n} \sim \frac{p}{q}$ implies $g\left(\frac{m}{n}\right) \sim g\left(\frac{p}{q}\right)$ for all $g \in \Gamma$, all Möbius maps in $\Gamma$ preserve Farey neighbors, and every Farey triangle in $\mathcal{F}$ is the image of $\mathbb{T}_0$ under some Möbius map in $\Gamma$. Using the given metric, every factor $t_k$ of $T$ preserves $\mathbb{H}$ and is an isometry of $\mathbb{H}$, with $d(u,v) = d(g(u), g(v))$ for all $u, v \in \mathbb{H}$. As parabolic Möbius maps, each $t_k$ is a conformal map that maps circles to circles [5] and Farey neighbors to Farey neighbors, properties which we use in our analysis.

### 2.3. The Convergence of Continued Fractions

In the work of Beardon [4], it is stated that convergence of the continued fraction of Equation (1) is equivalent to convergence of the sequence $S_n(0)$, where $S_n = s_0 s_1 \cdots s_n$ with $s_0(z) = b_0 + z$ and $s_n(z) = \frac{1}{b_n + z}$ for $n \in \mathbb{N}$. When using $T_n$ of Definition 3, convergence of the continued fraction of Equation (1) is equivalent to convergence of the sequence

$$T_0(0), T_1(\infty), T_2(0), T_3(\infty), T_4(0), T_5(\infty) \cdots .$$

From the work of Beardon [4], we state Pringsheim's Theorem without proof.

**Theorem 1.** *Suppose that for all $k$, $|b_k| \geq 1 + |a_k|$. Then the continued fraction* $\cfrac{a_1}{b_1 + \cfrac{a_2}{b_2 + \ddots}}$ *converges to some value $v$ with $|v| \leq 1$.*

The continued fraction of Equation (1) satisfies Theorem 1 if it is an $NICF$, as each $a_k = 1$ and each partial quotient $b_k$ is derived as the integer closest to $\frac{1}{\lfloor b_{k-1} \rceil - b_{k-1}}$, where $\lfloor b_{k-1} \rceil$ is the integer closest to $b_{k-1}$. Since $|\lfloor b_{k-1} \rceil - b_{k-1}| < \frac{1}{2}$ for each partial quotient of an $NICF$, all $|b_k| \geq 2$ and the $NICF$ of $\xi - b_0$ given by $\cfrac{1}{b_1 + \cfrac{1}{b_2 + \ddots}} = [0, b_1, b_2, \cdots]$ converges to a value between $-1$ and $1$.

## 3. Generating New Dynamics for the Continued Fraction

We use the images of the fundamental triangle $\mathbb{T}_0$ (with vertices 0, 1, and $\infty$) under the application of the consecutive partial products $T_n$, for $n \in \mathbb{N}_0$, to establish the geometry that underlies the process of using $RCF$s and $NICF$s to approximate real numbers.

**Example 1.** The $RCF$ and the $NICF$ for $\sqrt{5}-2 \approx 0.23606\ldots$ is $[0,4,4,4,4,\ldots] = [0,\overline{4}]$, from which we derive the product of parabolic maps

$$T = \tau_0\left(\phi\tau_4\phi\right)\tau_4\left(\phi\tau_4\phi\right)\tau_4\left(\phi\tau_4\phi\right)\cdots = \overline{\left(\phi\tau_4\phi\right)\tau_4}.$$

The convergents of $\sqrt{5}-2$ are

$$C_0 = 0, \quad C_1 = \frac{1}{4}, \quad C_2 = \frac{4}{17}, \quad C_3 = \frac{17}{72}, \cdots .$$

The diagram in Figure 2 shows all Farey triangles[1] crossed by the geodesic $\lambda_{\left(P,\sqrt{5}-2\right)}$ (from point $P$ on the imaginary axis to $\sqrt{5}-2$ on the real axis). We show the five Farey triangles that share a common vertex at each convergent. Each of these triangles is linked directly to the coefficients in the product of Möbius maps derived from the continued fraction as follows.

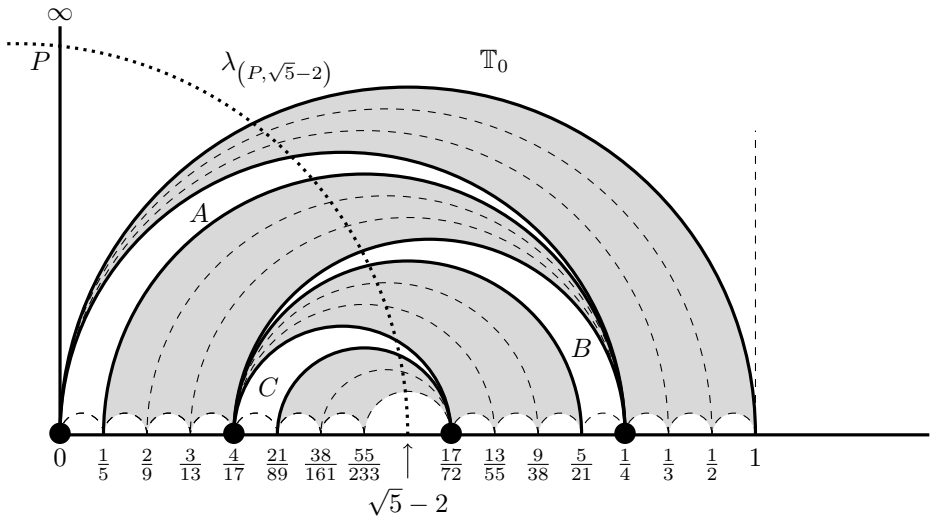


Figure 2: All Farey triangles cut by the geodesic $\lambda_{\left(P,\sqrt{5}-2\right)}$.

- For $C_0 = 0$: From point $P$, the geodesic $\lambda_{\left(P,\sqrt{5}-2\right)}$ first passes through the triangle $T_0\left(\mathbb{T}_0\right) = \mathbb{T}_0 = (0,1,\infty)$. The geodesic $\lambda_{\left(P,\sqrt{5}-2\right)}$ then passes through the three shaded triangles $\left(0,\frac{1}{2},1\right)$, $\left(0,\frac{1}{3},\frac{1}{2}\right)$, and $\left(0,\frac{1}{4},\frac{1}{3}\right)$, which are the

[1]The pair of ideal end points of each Farey geodesics represent a pair of Farey neighbors in $\mathbb{R}$. All Farey fractions that appear in the diagram of Figure 2 are drawn equidistant from each other. This adjustment in the diagram allows us to work with rational values that are very close to $\sqrt{5}-2$ more easily.

images of $\mathbb{T}_0$ under $(\phi\tau_1\phi)$, $(\phi\tau_2\phi)$ and $(\phi\tau_3\phi)$, respectively, to get to $T_1(\mathbb{T}_0) = (\phi\tau_4\phi)(\mathbb{T}_0) = \left(0, \frac{1}{5}, \frac{1}{4}\right)$, which is labeled $A$ in the diagram of Figure 2. Each of these Farey triangles has 0 as a vertex, since 0 is the image of the 0 vertex of $\mathbb{T}_0$ under each of the given maps. The vertex $\frac{1}{4}$ is the image of $\infty$ under $T_1 = \tau_0(\phi\tau_4\phi)$.

- For $C_1 = \frac{1}{4}$: Continuing from $T_1(\mathbb{T}_0) = \left(0, \frac{1}{5}, \frac{1}{4}\right)$, the geodesic $\lambda_{(P,\sqrt{5}-2)}$ passes through the three shaded triangles $\left(\frac{1}{5}, \frac{2}{9}, \frac{1}{4}\right)$, $\left(\frac{2}{9}, \frac{3}{13}, \frac{1}{4}\right)$, and $\left(\frac{3}{13}, \frac{4}{17}, \frac{1}{4}\right)$, which are the images of $\mathbb{T}_0$ under $(\phi\tau_4\phi)\tau_1$, $(\phi\tau_4\phi)\tau_2$ and $(\phi\tau_4\phi)\tau_3$, respectively, to get to $T_2(\mathbb{T}_0) = (\phi\tau_4\phi)\tau_4(\mathbb{T}_0) = \left(\frac{4}{17}, \frac{5}{21}, \frac{1}{4}\right)$, which is labeled $B$ in the diagram of Figure 2. Each of these Farey triangles has $\frac{1}{4}$ as a vertex, since $\frac{1}{4}$ is the image of the $\infty$ vertex of $\mathbb{T}_0$ under each of the given maps. The vertex $\frac{4}{17}$ is the image of 0 under $T_2 = \tau_0(\phi\tau_4\phi)\tau_4$.

This process continues indefinitely, matching each partial quotient '4' to the four Farey triangles generated under the associated partial product of Möbius maps $T_n$ for all $n \in \mathbb{N}$.

### 3.1. Fixed Points

As we build up successive images of $\mathbb{T}_0$ under the $T_n$ transformations, the images of 0 and $\infty$ are alternatively fixed points of the last map in the composition as the map $\tau_{b_n}$ fixes $\infty$ and $\phi\tau_{b_n}\phi$ fixes 0. Each iteration generates a fixed point with respect to the previous iteration. We define the fixed points under $T_n$ as follows.

**Definition 4.** Let $T_n$ be a partial product of parabolic Möbius maps. If $T_{n-1}(p) = T_n(p)$, $n \in \mathbb{N}$, then $T_n(p)$ is the *fixed point in the progression of triangles from* $T_{n-1}(\mathbb{T}_0)$ *to* $T_n(\mathbb{T}_0)$.

For each partial product of Möbius maps $T_n$, the value $T_n(0)$ is the fixed point in the progression of triangles from $T_{n-1}(\mathbb{T}_0)$ to $T_n(\mathbb{T}_0)$ when $n$ is odd, and the value $T_n(\infty)$ is the fixed point in the progression of triangles from $T_{n-1}(\mathbb{T}_0)$ to $T_n(\mathbb{T}_0)$ when $n$ is even.

### 3.2. Intermediate Farey Triangles

We define the intermediate images of $\mathbb{T}_0$ for each $T_n$ as follows.

**Definition 5.** In the partial product of Möbius maps $T_n = t_0t_1\cdots t_{n-1}t_n$, with $t_n = \tau_{b_n}$ for $n$ even and $t_n = \phi\tau_{b_n}\phi$ for $n$ odd, we replace $t_n$ with $t_k$ to get $T_{n,k} = t_0t_1\cdots t_{n-1}t_k$ (for all $1 \le k \le b_n - 1$, $k \in \mathbb{N}$), where $t_k = \tau_k$ for $n$ even and $t_k = \phi\tau_k\phi$ for $n$ odd. The Farey triangles $T_{n,k}(\mathbb{T}_0) = t_0t_1\cdots t_{n-1}t_k(\mathbb{T}_0)$, $k = 1, \ldots, b_n - 1$, are called the *intermediate Farey triangles between* $T_{n-1}(\mathbb{T}_0)$ *and* $T_n(\mathbb{T}_0)$.

**Example 2.** In the diagram of Figure 2, the shaded triangles

$$T_{1,1}(\mathbb{T}_0) = \left(0, \frac{1}{2}, 1\right), T_{1,2}(\mathbb{T}_0) = \left(0, \frac{1}{3}, \frac{1}{2}\right) \text{ and } T_{1,3}(\mathbb{I}_0) = \left(0, \frac{1}{4}, \frac{1}{3}\right)$$

share the vertex $T_1(0) = 0$, as it is the fixed point in the progression of triangles from $T_0(\mathbb{T}_0)$ to $T_1(\mathbb{T}_0)$. These three triangles are the three intermediate Farey triangles between $T_0(\mathbb{T}_0)$ and $T_1(\mathbb{T}_0)$.

### 3.3. The Link between Partial Quotients and Intermediate Farey Triangles

The following proposition states the link between partial quotients and the number of intermediate Farey triangles for each $T_n$.

**Proposition 1.** *For each $n \in \mathbb{N}$, there are $b_n - 1$ intermediate Farey triangles between $T_{n-1}(\mathbb{T}_0)$ and $T_n(\mathbb{T}_0)$, and each pair of consecutive intermediate triangles $T_{n,k-1}(\mathbb{T}_0)$ and $T_{n,k}(\mathbb{T}_0)$, share a common edge, for all $k \in \mathbb{N}$ with $1 < k \leq b_n - 1$.*

*Proof.* By simple calculation, we have that

$$\phi\tau_1\phi(0, 1, \infty) = \left(0, \frac{1}{2}, 1\right) \qquad \text{and} \qquad \tau_1(0, 1, \infty) = (1, 2, \infty),$$

so

$$T_{n,1}(0, 1, \infty) = T_{n-1}(\phi\tau_1\phi)(0, 1, \infty) = T_{n-1}\left(0, \frac{1}{2}, 1\right), \text{ for } n \text{ odd},$$

and

$$T_{n,1}(0, 1, \infty) = T_{n-1}\tau_1(0, 1, \infty) = T_{n-1}(1, 2, \infty), \text{ for } n \text{ even}.$$

Thus, with $v = 0$ for $n$ odd and $v = \infty$ for $n$ even, we have that $T_{n,1}(v) = T_{n-1}(v)$ and $T_{n,1}\left(\frac{1}{v}\right) = T_{n-1}(1)$. The Farey triangles $T_{n-1}(\mathbb{T}_0)$ and $T_{n,1}(\mathbb{T}_0)$ share the edge $T_{n-1}\left(\lambda_{v,\frac{1}{v}}\right) = T_{n,1}(\lambda_{v,1})$. Similarly, $T_{n,k}(v) = T_{n,k-1}(v)$ and $T_{n,k}\left(\frac{1}{v}\right) = T_{n,k-1}(1)$. Thus $T_{n,k-1}(\mathbb{T}_0)$ and $T_{n,k}(\mathbb{T}_0)$ share the edge $T_{n,k}\left(\lambda_{v,\frac{1}{v}}\right) = T_{n,k-1}(\lambda_{v,1})$ as required.

Since $1 < k \leq b_n - 1, k \in \mathbb{N}$, it follows that there are $b_n - 1$ intermediate Farey triangles between $T_{n-1}(\mathbb{T}_0)$ and $T_n(\mathbb{T}_0)$. □

## 4. Nearest Integer Continued Fractions with Negative Partial Quotients

For $n \in \mathbb{N}$, the continued fraction in Equation (1) has partial quotients $b_n$ that are natural numbers when it is an $RCF$, but integers when it is an $NICF$. We show the difference in the geometry when an $NICF$ has negative partial quotients.

**Example 3.** For $\sqrt{3}-1 \approx 0.73205\ldots$ the $RCF$ is $[0,\overline{1,2}]$ and the function $T_n$ becomes:

$$T_n(z) = \begin{cases} \tau_0\left(\phi\tau_1\phi\right)\tau_2\left(\phi\tau_1\phi\right)\cdots\left(\phi\tau_1\phi\right)\tau_2\left(\phi\tau_1\phi\right)(z), & \text{for } n \text{ odd} \\ \tau_0\left(\phi\tau_1\phi\right)\tau_2\left(\phi\tau_1\phi\right)\cdots\tau_2\left(\phi\tau_1\phi\right)\tau_2(z), & \text{for } n \text{ even} \end{cases} \tag{2}$$

where each product has $n+1$ factors. The values for $T_n(0)$, $T_n(1)$, and $T_n(\infty)$, calculated using Equation (2), are shown in Table 1. The corresponding $T_n\left(\mathbb{T}_0\right)$ are labeled in the diagram of Figure 3.

In the diagram of Figure 3, there is one shaded intermediate triangle between $T_n\left(\mathbb{T}_0\right)$ and $T_{n+1}\left(\mathbb{T}_0\right)$ for $n$ odd, and none between $T_n\left(\mathbb{T}_0\right)$ and $T_{n+1}\left(\mathbb{T}_0\right)$ for $n$ even, which satifies the link between partial quotients and the number of intermediate Farey triangles established in Proposition 1 in Section 3.3.

| $z$ | $T_0(z)$ | $T_1(z)$ | $T_2(z)$ | $T_3(z)$ | $T_4(z)$ | $T_5(z)$ | $T_6(z)$ |
|---|---|---|---|---|---|---|---|
| | $\tau_0$ | $\tau_0\left(\phi\tau_1\phi\right)$ | $\tau_0\left(\phi\tau_1\phi\right)\tau_2$ | $T_2\left(\phi\tau_1\phi\right)$ | $T_3\tau_2$ | $T_4\left(\phi\tau_1\phi\right)$ | $T_5\tau_2$ |
| 0 | 0 | 0 | 2/3 | 2/3 | 8/11 | 8/11 | 30/41 |
| 1 | 1 | 1/2 | 3/4 | 5/7 | 11/15 | 19/26 | 41/56 |
| $\infty$ | $\infty$ | 1 | 1 | 3/4 | 3/4 | 11/15 | 11/15 |

Table 1: The images of 0, 1, and $\infty$ under $T_n$ for $n = 0, \cdots, 6$.

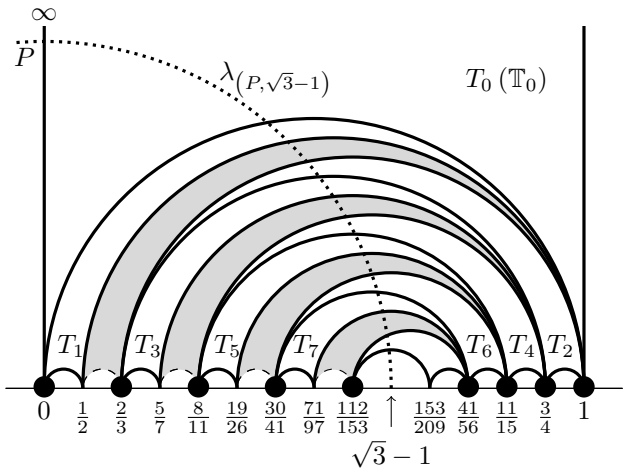


Figure 3: The images of $\mathbb{T}_0$ under successive $T_n$ derived from the $RCF$.

Using the nearest integer division algorithm for $\sqrt{3}-1$, we get the $NICF$

$$\sqrt{3}-1 = [1,-4,4,-4,4,...] = [1,\overline{-4,4}],$$

and Definition 3 gives us $T_n$ for the $NICF$ as follows:

$$T_n(z) = \begin{cases} \tau_1\left(\phi\tau_{-4}\phi\right)\tau_4\left(\phi\tau_{-4}\phi\right)\cdots\left(\phi\tau_{-4}\phi\right)\tau_4\left(\phi\tau_{-4}\phi\right)(z), & \text{for } n \text{ odd} \\ \tau_1\left(\phi\tau_{-4}\phi\right)\tau_4\left(\phi\tau_{-4}\phi\right)\cdots\tau_4\left(\phi\tau_{-4}\phi\right)\tau_4(z), & \text{for } n \text{ even} \end{cases} \tag{3}$$

where each product has $n+1$ factors. The values for $T_n(0)$, $T_n(1)$, and $T_n(\infty)$, calculated using Equation (3), are shown in Table 2. The corresponding $T_n\left(\mathbb{T}_0\right)$ are shaded in the diagram of Figure 4.

In the diagram of Figure 4, since there are three Farey triangles between $T_{n-1}\left(\mathbb{T}_0\right)$ and $T_n\left(\mathbb{T}_0\right)$ for each $n \in \mathbb{N}$, we see that the link between the $b_n$ (the partial quotients of the $NICF$) and the number of intermediate Farey triangles (between $T_{n-1}\left(\mathbb{T}_0\right)$ and $T_n\left(\mathbb{T}_0\right)$) still satisfies Proposition 1 in Section 3.3.

| $z$ | $T_0(z)$ | $T_1(z)$ | $T_2(z)$ | $T_3(z)$ | $T_4(z)$ | $T_5(z)$ |
|---|---|---|---|---|---|---|
| | $\tau_1$ | $\tau_1\left(\phi\tau_{-4}\phi\right)$ | $\tau_1\left(\phi\tau_{-4}\phi\right)\tau_4$ | $T_2\left(\phi\tau_{-4}\phi\right)$ | $T_3\tau_4$ | $T_4\left(\phi\tau_{-4}\phi\right)$ |
| 0 | 1 | 1 | 11/15 | 11/15 | 153/209 | 153/209 |
| 1 | 2 | 2/3 | 14/19 | 30/41 | 194/245 | $\cdots$ |
| $\infty$ | $\infty$ | 3/4 | 3/4 | 41/56 | 41/56 | $\cdots$ |

Table 2: The images of 0, 1, and $\infty$ under $T_n$ for $n = 0, \cdots, 5$.

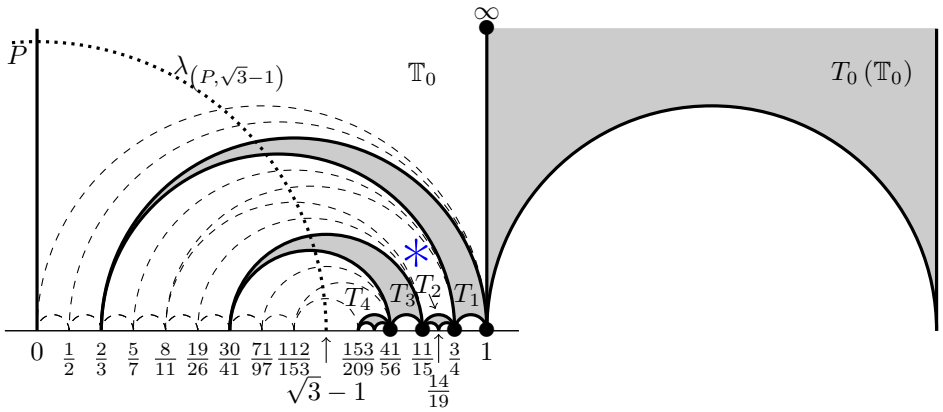


Figure 4: The images of $\mathbb{T}_0$ under successive $T_n$ derived from the $NICF$.

This result, however, is not as satisfactory in the case of the $NICF$ as it is in the case of the $RCF$ for the following two reasons.

i) The vertices of $T_2\left(\mathbb{T}_0\right) = \left(\frac{3}{4}, \frac{14}{19}, \frac{11}{15}\right)$ are all larger than $\sqrt{3}-1$.

ii) The Farey triangle marked with the $^*$, in the diagram of Figure 4, is the third intermediate triangle $\left(T_{2,3}\left(\mathbb{T}_0\right)\right)$ between $T_1\left(\mathbb{T}_0\right)$ and $T_2\left(\mathbb{T}_0\right)$, but it is also

the first intermediate triangle ($T_{3,1}(\mathbb{T}_0)$) between $T_2(\mathbb{T}_0)$ and $T_3(\mathbb{T}_0)$, which means that this Farey triangle is a repeated image among the intermediate Farey triangles of the product of parabolic Möbius maps in the $T_n$ derived from the $NICF$.

The two conditions, where all vertices of the Farey triangle are larger than the target and Farey triangles are repeated, occur for all even values of $n$ in this example. However, it is clear from Tables 1 and 2 that the $NICF$ produces approximants with greater speed.

We avoid the problems of 'all vertices larger than target' and 'repeated images', as seen in the $NICF$ of Example 3, by recognizing and isolating the elliptic Möbius maps from the parabolic Möbius maps in $T_n$.

## 5. Dynamics Generated by the NICF

For the product of parabolic Möbius maps derived from the $NICF$ we introduce the following notation. The parabolic Möbius maps that fix $\infty$ and 0 are

$$p_\infty = \tau_1 \text{ and } p_0 = (\phi\tau_1\phi),$$

respectively. The elliptic Möbius maps are

$$s = \tau_1(\phi\tau_{-1}\phi), \text{ and its inverse } s^{-1} = (\phi\tau_1\phi)\tau_{-1}.$$

In the following theorem, we show that $s$ and $s^{-1}$ act as elliptic Möbius maps on $\mathbb{H}$ and summarize the procedure for finding and isolating the elliptic maps in the product of parabolic Möbius maps of Definition 3.

**Theorem 2.** *The maps $s$ and $s^{-1}$ are maps of order 3 that permute the vertices 0, 1, and $\infty$. The maps $s$ and $s^{-1}$ are the only elliptic maps found among the factors of the product of parabolic Möbius transformations generated from an $NICF$.*

*Proof.* The maps $s$ and $s^{-1}$ both appear among the factors of the product of parabolic Möbius maps as a product of two parabolic maps, $p_\infty p_0^{-1} = \tau_1(\phi\tau_{-1}\phi)$ and $p_0 p_\infty^{-1} = (\phi\tau_1\phi)\tau_{-1}$, which are $s$ and $s^{-1}$, respectively.

A simple calculation shows both $s$ and $s^{-1}$ fix the single point $\dfrac{1+\sqrt{3}i}{2}$ in $\mathbb{H}$. The calculations

$$s(0) = 1, s(1) = \infty, s(\infty) = 0 \text{ and } s^{-1}(0) = \infty, s^{-1}(1) = 0, s^{-1}(\infty) = 1$$

show that $s$ and $s^{-1}$ are maps of order 3 that permute the vertices 0, 1, and $\infty$.

We express

$$T_n(z) = \begin{cases} \tau_{b_0}(\phi\tau_{b_1}\phi)\tau_{b_2}(\phi\tau_{b_3}\phi)\cdots\left(\phi\tau_{b_{n-2}}\phi\right)\tau_{b_{n-1}}(\phi\tau_{b_n}\phi)(z), & \text{for } n \text{ odd} \\ \tau_{b_0}(\phi\tau_{b_1}\phi)\tau_{b_2}(\phi\tau_{b_3}\phi)\cdots\tau_{b_{n-2}}\left(\phi\tau_{b_{n-1}}\phi\right)\tau_{b_n}(z), & \text{for } n \text{ even,} \end{cases} \tag{4}$$

derived from the $NICF$, in terms of the Möbius maps $p_0$, $p_\infty$, $s$ and $s^{-1}$ as follows. Clearly the map $\phi\tau_{b_n}\phi$ can be writen as $\phi\tau_{\pm1}\tau_{b_n}\tau_{\mp1}\phi = (\phi\tau_{\pm1+b_n}\phi)(\phi\tau_{\mp1}\phi) = (\phi\tau_{\pm1}\phi)(\phi\tau_{b_n\mp1}\phi)$ since $\phi^2$ and $\tau_{\pm1\mp1} = \tau_0$ are both the identity map. Anywhere in the product $T_n(z)$ where $b_k > 0$ and $b_{k+1} < 0$, we rearrange the factors involving $b_k$ and $b_{k+1}$, and make the elliptic Möbius maps explicit. There are two cases.

- When $k$ is even, the factors $\cdots\tau_{b_k}\left(\phi\tau_{b_{k+1}}\phi\right)\cdots$ are rearranged to become $\cdots\tau_{b_k-1}\left[\tau_1\left(\phi\tau_{-1}\phi\right)\right]\left(\phi\tau_{b_{k+1}+1}\phi\right)\cdots$ which is equal to $\cdots p_\infty^{b_k-1}sp_0^{b_{k+1}+1}$.
- When $k$ is odd, the factors $\cdots\left(\phi\tau_{b_k}\phi\right)\tau_{b_{k+1}}\cdots$ are rearranged to become $\cdots\left(\phi\tau_{b_k-1}\phi\right)\left[\left(\phi\tau_1\phi\right)\right]\tau_{-1}]\tau_{b_{k+1}+1}\cdots$ which is equal to $\cdots p_0^{b_k-1}s^{-1}p_\infty^{b_{k+1}+1}$.

After that, all remaining $(\phi\tau_b\phi)$ are replaced with $p_0^b$ and all remaining $\tau_b$ are replaced with $p_\infty^b$ to produce the product of Möbius maps called $T_M$. The product $T_n$ derived from the $NICF$ yields only $s$ and $s^{-1}$ as elliptic factors. □

In Example 4, we show that the use of Möbius maps allows us to identify new geometrical aspects embedded in the process of finding rational approximants using continued fractions.

**Example 4.** For $\sqrt{3}-1$, we replace $T = \tau_1\left(\phi\tau_{-4}\phi\right)\tau_4\left(\phi\tau_{-4}\phi\right)\cdots$ for $\sqrt{3}-1$ with the product of Möbius maps

$$T = \left[\tau_1\left(\phi\tau_{-1}\phi\right)\right]\left(\phi\tau_{-3}\phi\right)\tau_3[\tau_1\left(\phi\tau_{-1}\phi\right)]\left(\phi\tau_{-3}\phi\right)\tau_3[\tau_1\left(\phi\tau_{-1}\phi\right)]\cdots, \tag{5}$$

which becomes

$$T_M = sp_0^{-3}p_\infty^3sp_0^{-3}p_\infty^3sp_0^{-3}p_\infty^3\cdots \tag{6}$$

or more simply

$$T_M = \overline{sp_0^{-3}p_\infty^3}. \tag{7}$$

The partial products derived from Equation (7) are

$$T_{M(n)} = sp_0^{-3}p_\infty^3sp_0^{-3}p_\infty^3sp_0^{-3}p_\infty^3\cdots t_{M(n)},$$

where $t_{M(n)}$ represents the $nth$ factor in the product of Möbius maps $T_M$. We now track the images of the vertices 0, 1, and $\infty$ of $\mathbb{T}_0$ under the application of successive $T_{M(n)}$.

Each line under the diagram of Figure 5 shows the images of $\mathbb{T}_0$ under successive $T_{M(n)}$ where $T_{M(1)} = s$, $T_{M(2)} = sp_0^{-3}$, $T_{M(3)} = sp_0^{-3}p_\infty^3$, $T_{M(4)} = sp_0^{-3}p_\infty^3s$ and so on. We show the movement of images of $\mathbb{T}_0$ under the $T_{M(n)}$ generated from the $NICF$ using maps $p_0$ and $p_\infty$ next to the arrow that represents the movement that they cause in the diagram of Figure 5. An $s$ is placed in the triangle whose vertices have been permuted by the $s$ map. The effects of $T_{M(2)}$ and $T_{M(3)}$ are elaborated over three lines below the image.

For each progression shown in the diagram of Figure 5 under successive $T_{M(n)}$, we describe the associated movement as follows.

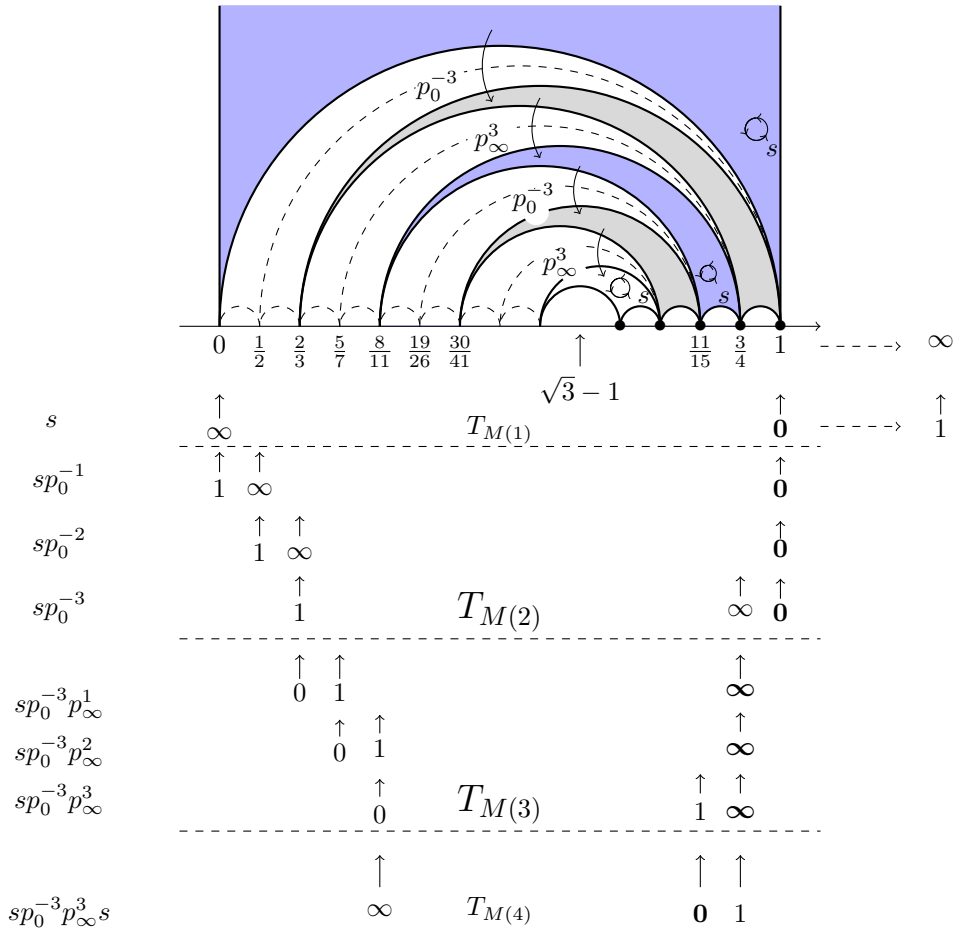


Figure 5: Tracing the iterates $T_{M(n)}(0)$, $T_{M(n)}(1)$ and $T_{M(n)}(\infty)$ for the $NICF$ of $\sqrt{3}-1$ to count movements of triangles about fixed points for $\sqrt{3}-1$.

- Start with the vertices 0, 1, and $\infty$ of $\mathbb{T}_0$.
- For $T_{M(1)}$: Of the three vertices, 0, 1, and $\infty$, 1 is the closest to $\xi$, so we permute the vertices using $s$. In the line with $s$ on the left hand side in the diagram of Figure 5, we note that images of 0, 1, and $\infty$ are the three vertices permuted by $T_{M(1)} = s$, so $s(\infty) = 0$ and $s(0) = 1$. Here $s(1) = \infty$ as indicated.
- For $T_{M(2)}$: The image of 0 under $T_{M(1)}$ is now closest to the target $\xi$, so it should be fixed under $t_2$. Since $t_2 = \phi\tau_{-3}\phi$, the image of 0 is fixed under $T_{M(2)}$ as illustrated by the next three lines in the diagram of Figure 5, while

the images of 1 and $\infty$ approach $T_{M(1)}(0) = T_{M(2)}(0) = 1$ from the left.

- For $T_{M(3)}$: The image of $\infty$ under $T_{M(2)}$ is closest to $\xi$, and this point will be fixed by $t_3 = \tau_3$. The images of 0 and 1 approach $T_{M(2)}(\infty) = T_{M(3)}(\infty) = \frac{3}{4}$ from the left under $T_{M(2)}$ as shown in the next three lines in the diagram of Figure 5.
- For $T_{M(4)}$: After the last iteration, $T_{M(3)}(1)$ is closest to $\xi$. The map $s$ is used again to permute the images of 0, 1, and $\infty$. The vertex $T_{M(4)}(0)$ is now closest to $\xi$ and the process is continued in the same way.

Example 4 serves to highlight the new roles adopted by vertices, geodesics and Farey triangles in the process of generating approximations. Changing the focus from the $RCF$ to the $NICF$ changes the following parts of the process.

- The Euclidean division algorithm is replaced by the nearest integer division algorithm.
- Reading off values of partial quotients of the $RCF$ is replaced by an analysis of Möbius maps derived from the $NICF$, requiring that we separate the elliptic maps $s$ and $s^{-1}$ from the parabolic maps.
- Counting left and right cuts along a geodesic is replaced by counting movements of hyperbolic triangles about successive fixed points.

## 6. Partial Quotients and the Link between Adjusted Coefficients and Counting Triangles

In order to simplify the link between coefficients in $T_M$ and triangles in the Farey tessellation, we define the adjusted product as follows.

**Definition 6.** Let $b_n^*$ be the adjusted coefficient of the partial quotient $b_n$ after all the elliptic factors $s$ and $s^{-1}$ have been accommodated in the factors of $T$ to form $T_M$. The *adjusted product of $T$ for the $NICF$* is $T_A = t_0^* t_1^* t_2^* \cdots$, where each $t_n^*, n \in \mathbb{N}_0$ is a product of an elliptic map ($e$ (the identity map), $s$, or $s^{-1}$) and a parabolic map $\tau_{b_n^*}$ or $\phi\tau_{b_n^*}\phi$. The *partial adjusted product of $T$ for the $NICF$* is $T_{A_n} = t_0^* t_1^* t_2^* \cdots t_n^*$.

In the following example, we show the adjusted product of $\sqrt{3}-1$ of Example 4, in comparison with the original product of parabolic Möbius maps $T$.

**Example 5.** For $\sqrt{3}-1$:

$$\begin{array}{rcccccc} T & = & \tau_1 & (\phi\tau_{-4}\phi) & \tau_4 & (\phi\tau_{-4}\phi) & \cdots, \\ T_A & = & \tau_0 & s\,(\phi\tau_{-3}\phi) & \tau_3 & s\,(\phi\tau_{-3}\phi) & \cdots \\ & = & p_\infty^0 & s p_0^{-3} & p_\infty^3 & s p_0^{-3} & \cdots. \end{array}$$

Each coefficient is adjusted by the factor $s$ wherever it is accommodated.

When using continued fractions to find rational approximations of irrational reals, the $RCF$ is useful to get the configuration of the Farey triangles for the irrational number, but the $NICF$ gives us a quicker method to find approximations. By reinterpreting the Möbius maps of the $NICF$, we become aware of the roles of the images of 0, 1, and $\infty$. Using the partial product $T_{M(n)} = t_1 t_2 \cdots t_n$ it is easy to establish which of the three images is closest to the target by looking at $t_{n+1}$.

- If $t_{n+1} = p_\infty^b$ then $T_{M(n)}(\infty)$ is closest to the target and becomes the fixed point of $T_{M(n+1)}$.
- If $t_{n+1} = p_0^b$ then $T_{M(n)}(0)$ is closest to the target and becomes the fixed point of $T_{M(n+1)}$.
- If $t_{n+1} = s$ or $t_{n+1} = s^{-1}$ then $T_{M(n)}(1)$ is closest to the target. Since neither of the parabolic maps uses 1 as a fixed point the images of 0, 1, and $\infty$ must be permuted.

In the final example, we see the 'semi-periodic' pattern of the partial quotients associated with the number $e$. We give the conversion from the product of maps $T$ to the adjusted product of Möbius maps $T_A$ for $e - 2$.

**Example 6.** For $e - 2$ we have:

$$\begin{aligned}
T = \;& \tau_1 \quad (\phi\tau_{-4}\phi) \quad \tau_2 \quad (\phi\tau_5\phi) \quad \tau_{-2} \quad (\phi\tau_{-7}\phi) \quad \tau_2 \quad (\phi\tau_9\phi) \quad \tau_{-2}\cdots, \\
T_A = \;& \tau_0 \quad s\,(\phi\tau_{-3}\phi) \quad \tau_2 \quad (\phi\tau_4\phi) \quad s^{-1}\tau_{-1} \quad (\phi\tau_{-7}\phi) \quad \tau_2 \quad (\phi\tau_8\phi) \quad s^{-1}\tau_{-1}\cdots \\
= \;& p_\infty^0 \quad sp_0^{-3} \quad p_\infty^2 \quad p_0^4 \quad s^{-1}p_\infty^{-1} \quad p_0^{-7} \quad p_\infty^2 \quad p_0^8 \quad s^{-1}p_\infty^{-1}\cdots.
\end{aligned}$$

All fractions on the number line in the diagram of Figure 6 are approximations derived from the process of Farey subdivision [8], while the fractions $\frac{0}{1}, \frac{1}{1}, \frac{2}{3}, \frac{3}{4}, \frac{5}{7}, \cdots$ (connected with solid geodesics) are convergents of the $RCF$. Approximations that are marked by bullets in the diagram of Figure 6 are convergents of the $NICF$. The exponents of the $p_\infty$ and $p_0$ give the number of triangles that we move through about each fixed point, under successive $T_{M(n)}$ derived from the $NICF$, and the sign of the exponent indicates the direction of the movement for the triangles about the fixed point.

Once the Möbius maps for the $NICF$ of $\xi$ are established, the adjustment to the exponents of $p_\infty$ and $p_0$, when incorporating the maps $s$ and $s^{-1}$ to form the product $T_M$, ensure that the following theorem is satisfied.

**Theorem 3.** *For the product of Möbius maps $T_M$, derived from the $NICF$, the partial products of Möbius maps $T_{M(n)}$ generate images of the fundamental triangle $\mathbb{T}_0$ where*

*a) the exponents of $p_\infty$ and $p_0$ count triangles that each share the fixed point of a parabolic map as a common vertex;*

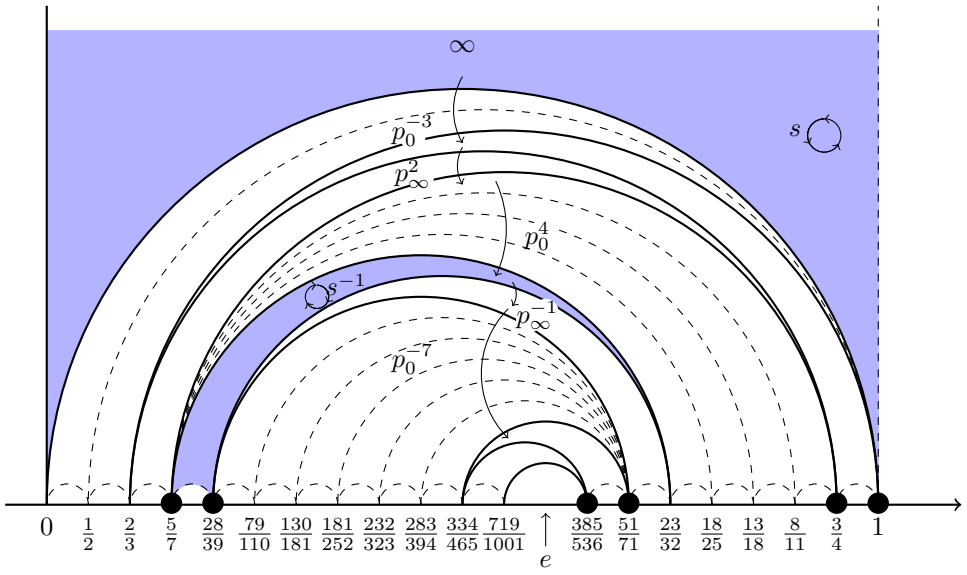


$$T_{M(n)} = sp_0^{-3}p_\infty^2p_0^4s^{-1}p_\infty^{-1}p_0^{-7}p_\infty^2p_0^8s^{-1}p_0^{-1}p_\infty^{-11}p_\infty^2p_0^{12}s^{-1}\cdots$$

Figure 6: Tracking images of $\mathbb{T}_0$ for $e-2$.

*b) the target $\xi$ lies between the smallest and the largest of the 3 vertices $T_{M(n)}(0)$, $T_{M(n)}(1)$, and $T_{M(n)}(\infty)$ of triangle $T_{M(n)}(\mathbb{T}_0)$, if $t_{M(n)}$ is equal to either $p_\infty$ or $p_0$, raised to a non-zero integer;*

*c) the 3 vertices $T_{M(n)}(0)$, $T_{M(n)}(1)$, and $T_{M(n)}(\infty)$ of triangle $T_{M(n)}(\mathbb{T}_0)$ are permuted if the map $t_{M(n+1)}$ is equal to $s$ or $s^{-1}$.*

This result establishes the link between the partial quotients of the $NICF$ and the number of triangles encountered in the Farey tessellation near $\xi$ in the same way that Series [12, 13] and Schmidt [11, page 18] did for the regular continued fraction.

## 7. Conclusion

The understanding of how a process works is often linked to the images we use to visualize the process. In the case of continued fractions, the dominant images are those that involve the regular continued fraction. This paper offers insight into the procedure for using the nearest integer continued fraction. The interpretation uses Möbius maps to maintain the level of accuracy for approximations of real numbers

using the $NICF$.

The examples so far have all had periodic or semi-periodic partial quotients in their $NICF$s. The $RCF$ of $\pi$ (given by $[3, 7, 15, 1, 292, 1, 1, \dots]$) and the $NICF$ of $\pi$, have no pattern for their partial quotients. Is there a way to extend the geometrical method of this paper to any of the well known, beautifully patterned continued fractions for $\pi$? For instance:

$$\pi = 3 + \cfrac{1^2}{6 + \cfrac{3^2}{6 + \cfrac{5^2}{6 + \cdots}}} \quad \text{and, from [10],} \quad \frac{\pi}{2} = 1 + \cfrac{1}{1 + \cfrac{1}{\frac{1}{2} + \cfrac{1}{\frac{1}{3} + \cdots}}}.$$

The geometry for continued fractions with numerators not all equal to 1, and those with numerators equal to 1, but denominators rational, need to be explored further.

As we extend work on continued fractions to higher dimensions, the $NICF$ provides a more viable option, so it is essential that we have suitable images that illustrate the underlying process of the $NICF$. In higher dimensions, simply truncating the $NICF$ has a negative impact on accuracy of the approximations. In the case of approximating reals, we already need to track the orbits of three vertices (namely $\infty$, 0, and 1) to visualize the process. As we move into approximating complex numbers using $NICF$s the number of vertices whose orbits we need to track increases. This will be the subject of our next paper. Thereafter we will explore the extension of these ideas to the approximation of quaternion numbers.

## References


[1] J. W. Anderson, *Hyperbolic Geometry*, Springer-Verlag, London, 2005.

[2] A. F. Beardon, *The Geometry of Discrete Groups*, Springer, Berlin, 1983.

[3] A. F. Beardon, Continued fractions, discrete groups and complex dynamics, *Comput. Methods Funct. Theory* **1** (2001), 535-594.

[4] A. F. Beardon, The geometry of Pringheim's continued fractions, *Geom. Dedicata* **84** (2001), 125-134.

[5] A. F. Beardon, *Algebra and Geometry*, Cambridge, Cambridge University Press, 2005.

[6] A. F. Beardon, Möbius maps and periodic continued fractions, *Math. Mag.* **88** (2015), 272-277.

[7] D. Hensley, *Continued Fractions*, World Scientific Publishing Co. Pte. Ltd., Hackensack, NJ, 2006.

[8] M. Hockman, Continued fractions and the geometric decomposition of modular transformations, *Quaest. Math.* **29** (2006), 427-446.

[9] M. Hockman and R. Van Rensburg, Simple continued fractions and cutting sequences, *Quaest. Math.* **36** (2013), 437-448.

[10] E. Scheinerman, T. J. Pickett and A. Coleman, Another continued fraction for $\pi$, *Amer. Math. Monthly* **115** (2008), 930-933.

[11] A. L. Schmidt, Diophantine approximation of complex numbers, *Acta Math.* **134** (1975), 1-85.

[12] C. Series, The modular surface and continued fractions, *J. Lond. Math. Soc. (2)* **2** (1985), 69-80.

[13] C. Series, The geometry of Markoff numbers, *Math. Intelligencer* **7** (1985), 20-28.